

AperTO - Archivio Istituzionale Open Access dell'Università di Torino

Electrochemistry of *Canis familiaris* cytochrome P450 2D15 with gold nanoparticles: An alternative to animal testing in drug discovery

This is the author's manuscript

Original Citation:

Availability:

This version is available <http://hdl.handle.net/2318/1528389> since 2019-03-12T14:06:24Z

Published version:

DOI:10.1016/j.bioelechem.2015.03.012

Terms of use:

Open Access

Anyone can freely access the full text of works made available as "Open Access". Works made available under a Creative Commons license can be used according to the terms and conditions of said license. Use of all other works requires consent of the right holder (author or publisher) if not exempted from copyright protection by the applicable law.

(Article begins on next page)



UNIVERSITÀ DEGLI STUDI DI TORINO

1

2

3

4 This is the accepted version of the following article:

5

6 [Francesco Rua, Sheila J. Sadeghi, Silvia Castrignanò, Francesca Valetti, and Gianfranco Gilardi.
7 Electrochemistry of *Canis familiaris* cytochrome P450 2D15 with gold nanoparticles: an alternative to
8 animal testing in drug discovery. *Bioelectrochemistry* (2015) 105: 110-116.],

9

10 which has been published in final form at
11 [<http://www.sciencedirect.com/science/article/pii/S1567539415000766>]

12

13 **Electrochemistry of *Canis familiaris* cytochrome P450 2D15 with gold**
14 **nanoparticles: an alternative to animal testing in drug discovery**

15
16 **Francesco Rua^a, Sheila J. Sadeghi^{a,b}, Silvia Castrignanò^a, Francesca Valetti^a, and Gianfranco**
17 **Gilardi^{a,b,*}**

18
19 ^aDepartment of Life Sciences and Systems Biology, University of Torino, Italy.

20 ^bCentre for Nanostructured Interfaces and Surfaces, University of Torino, Italy.

21
22
23
24 **CORRESPONDING AUTHOR**

25 * Gianfranco Gilardi, Department of Life Sciences and Systems Biology, Via Accademia Albertina
26 13, 10123 Turin, Italy. Phone: +39-011-6704593, Fax: +39-011-6704643, E-mail:
27 gianfranco.gilardi@unito.it

28
29
30
31 **ABSTRACT**

32 This work reports for the first time the direct electron transfer of the *Canis familiaris* cytochrome
33 P450 2D15 on glassy carbon electrodes to provide an analytical tool as an alternative to P450
34 animal testing in the drug discovery process. Cytochrome P450 2D15, that corresponds to the
35 human homologue P450 2D6, was recombinantly expressed in *Escherichia coli* and entrapped on
36 glassy carbon electrodes (GC) either with the cationic polymer polydiallyldimethylammonium
37 chloride (PDDA) or in presence of gold nanoparticles (AuNPs). Reversible electrochemical signals
38 of P450 2D15 were observed with calculated midpoint potentials ($E_{1/2}$) of -191 ± 5 and -233 ± 4 mV
39 vs Ag/AgCl for GC/PDDA/2D15 and GC/AuNPs/2D15, respectively.

40 These experiments were then followed by the electro-catalytic activity of the immobilized enzyme
41 in presence of metoprolol. The latter drug is a beta-blocker used for the treatment of hypertension
42 and is a specific marker of the human P450 2D6 activity. Electrocatalysis data showed that only in
43 the presence of AuNPs the expected α -hydroxy-metoprolol product was present as shown by HPLC.
44 The successful immobilization of the electroactive *Canis familiaris* cytochrome P450 2D15 on
45 electrode surfaces addresses the ever increasing demand of developing alternative *in vitro* methods
46 for a more detailed study of animal P450 enzymes' metabolism, reducing the number of animals
47 sacrificed in preclinical tests.

48
49
50
51
52
53 **KEYWORDS**

54 CYP, animal testing, carbon electrode, gold nanoparticle, immobilization, metoprolol.

1. Introduction

In view of the huge numbers of animals used during preclinical tests in drug discovery [1], both the European Union (European Commission and European Parliament, Directive 2010/63/EU) [2-3] and the US Food and Drug Administration (FDA) [4] are strongly supporting the development of alternative *in vitro* methods to implement the three Rs, that is “reduce, refine and replace” animal models [5].

Hepatic cytochromes P450 are central to toxicological studies due to their primary role in phase I metabolism of more than 80% of marketed drugs [6]. However to date, very little data is published on comparative *in vivo* interspecies studies with even less data available on the different animal P450 expression and/or their metabolic profile [7-10]. To this end, a fast and reliable *in vitro* method would offer the possibility of a more detailed study of the interaction of new drugs with the animal P450 enzymes therefore increasing the predictive value of these preclinical trials.

Canis familiaris is one of the most widely studied animal models used in safety determination of new pharmaceuticals [11-12] and, although the major isoforms of the human cytochromes P450 2D6, 3A4, 2E1, 2C19 and 1A2 have been identified in *C. familiaris* [13-16], there is still a lack of knowledge on their pharmacogenomic/metabolic diversity [9].

Electrochemical techniques already developed in our lab for human hepatic monooxygenases including cytochromes P450 [17-22] represent the ideal approach for a sensitive, accurate and rapid evaluation of animal P450-drug interactions obviating both the requirement for a redox partner and the addition of NADPH cofactor as already reported for some animal P450 enzymes recombinantly expressed in a soluble form [23-25].

In this work, *Canis familiaris* P450 2D15 was chosen as a model for the investigation of canine cytochromes P450 by adopting electrochemical approaches to provide a method for the screening of the safety of new chemical entities/drugs. This enzyme shares 75% identity with the human cytochrome P450 2D6 which alone is responsible for the metabolism of 20–25% of commonly used therapeutic drugs including antiarrhythmics, adrenoceptor antagonists, and tricyclic antidepressants [6, 26]. The high P450 2D6 polymorphism profile is strictly related to either adverse drug reactions or no drug response [26-27] and to date six different variants have been already identified in the corresponding homologous *C. familiaris* P450 2D15 [28-30].

Generally, the study of the catalytic properties of canine P450 2D enzymes is hampered by the difficulty in their preparation from liver microsomes [14] or by their recombinant expression and purification in a stable form when not associated to the membranes [14-15, 28, 30]. To this end, in this work we report for the first time the recombinant expression and purification of the *Canis familiaris* P450 2D15 in a N-terminally modified form maintaining its structural integrity and function. Furthermore, the electrocatalytic functionality of the purified enzyme is tested whilst immobilized on glassy carbon electrodes (GC).

Two different immobilization strategies were adopted: a) entrapment within the cationic polymer polydiallyldimethylammonium chloride (PDDA) (GC/PDDA/2D15); b) immobilization in presence of gold nanoparticles (AuNPs) stabilized with didodecyldimethylammonium bromide (DDAB) (GC/AuNPs/2D15). Gold nanoparticles are widely used in electrochemical applications [31] especially because they act as excellent electron transfer relays by enhancing the electron transfer from the electrode to the protein [32].

Electrochemical properties of *C. familiaris* P450 2D15 immobilized on glassy carbon electrodes were characterized by cyclic voltammetry and the activity of this enzyme in presence of metoprolol, a selective β_1 receptor blocker used in treatment of cardiovascular disease and a marker for human P450 2D6 activity, assayed by chronoamperometry. The separation and identification of the product

105 formed was carried out by HPLC leading to the calculation of the K_M value of metoprolol for the
106 first time through the electrochemical system GC/AuNPs/2D15.

107
108

109 **2 Material and methods**

110 **2.1 Reagents**

111 Kits for plasmid and gene purification were purchased from Sigma Aldrich (Italy). Restriction
112 enzymes, T4 DNA ligase, Vent Polymerase and dNTPS were from New England Biolabs (UK).
113 Chromatographic resins were purchased from GE healthcare (Italy). Quinidine ((S)-[(2R,4S,5R)-5-
114 ethenyl-1-azabicyclo[2.2.2]octan-2-yl](6-methoxyquinolin-4-yl)methanol) and (±)-Metoprolol ({2-
115 hydroxy-3-[4-(2-methoxyethyl)phenoxy]propyl}(propan-2-yl)amine) (+)-tartrate salt, racemic
116 mixture, were purchased from Sigma Aldrich (Italy). Analytical grade chemicals tetrachloroauric
117 (III) acid (gold(III) chloride), DDAB (didodecyl-dimethylammonium bromide) and PDDA
118 (poly(dimethyldiallylammonium chloride)) were all purchased from Sigma-Aldrich and their
119 solutions prepared prior to their use in appropriate solvent for electrochemical experiments.

120

121 **2.2 Cloning of recombinant P450 2D15**

122

123 The gene coding for cytochrome P450 2D15 was amplified from the liver cDNA of *C. familiaris*
124 (Biochain, UK) using the primers Fw: 5'-AGACAGCTATGGGGCTGCTG-3' and Rv: 5'-
125 TGGTTTATTGTACCTCGGGCC-3'. The entire gene was blunt end ligated into pBS SK II(+)
126 cloning vector using the *EcoRV* restriction enzyme.

127 Subsequently, the full-length cDNA coding for the canine P450 was cloned into a pCW expression
128 vector [33] fused in frame with the sequence coding for the leader peptide of the bacterial OmpA
129 protein (MKKTAIAIAVALAGFATVAQA). This system has been previously used to enhance the
130 expression of native mammalian cytochromes P450 in *E. coli* [14, 34]. This leader peptide is
131 cleaved in the bacterial membrane to yield the native P450 enzymes. A code of four histidine
132 residues was added at the C-terminus before the STOP codon to facilitate the protein purification by
133 affinity chromatography.

134

135 **2.3 Expression and purification of *C. familiaris* P450 2D15**

136

137 Large-scale expression (4 liters) of P450 2D15 in *E. coli* DH5 α cells transformed with pCW- 2D15
138 was carried out as described previously for other P450 cytochromes [35] decreasing the post-
139 induction expression time and temperature to 24 hours and 24 °C, respectively.

140 Purification of P450 2D15 was carried out starting from the isolated membrane fraction using an
141 anion exchange DEAE sepharose column (GE-healthcare, Italy) and followed by a nickel ion
142 affinity chromatography step (GE-healthcare, Italy) where the protein remained bound through the
143 engineered His-tag and subsequently eluted using a 0–40 mM linear gradient of histidine. In order
144 to preserve the P450 2D15 stability the protein was purified in presence of the human P450 2D6
145 inhibitor quinidine [36]. The UV-visible spectra of the oxidized, reduced and reduced-carbon
146 monoxide bound forms of the protein were recorded on a Hewlett-Packard 8453 diode array
147 spectrophotometer. The P450 concentration was calculated by the method described by Omura and
148 Sato [37].

149

150 **2.4 Synthesis of AuNPs**

151

152 DDAB stabilized AuNPs were synthesized following the procedure described by Castrignanò et al.
153 in 2012 [32]. In particular, 0.5 mL of 10 mM tetrachloroauric (III) acid aqueous solution were

154 mixed under vigorous stirring to 1 mL of a chloroform 0.1 M DDAB solution for 20 minutes to
155 allow the complete transfer of Au(III) ions from the aqueous to the chloroform. After the two
156 phases were separated, 0.2 mL of freshly prepared aqueous solution of 0.4 M sodium borohydride
157 were slowly added. After additional two hours of vigorous stirring, the red organic phase containing
158 the DDAB stabilized AuNPs was collected and stored at 4 °C before use. TEM morphological
159 characterization showed that the synthesized DDAB stabilized AuNPs mainly consist of spherical
160 particles of about 6.5-8.5 nm diameter, ranging from 2.5 to 13 nm in size.

161

162 ***2.5 Immobilization of P450 2D15 on glassy carbon electrode and electrochemical measurements***

163

164 All electrochemical experiments were carried out at room temperature (25 °C) and in 50 mM
165 phosphate buffer pH 7.4, containing 100 mM KCl as supporting electrolyte, using an Autolab
166 PGSTAT12 potentiostat (Ecochemie, The Netherlands) controlled by GPES3 software. A
167 conventional three-electrode glass cell of 0.5 mL volume, equipped with a platinum wire counter
168 electrode, an Ag/AgCl (3 M NaCl) reference electrode and 3 mm diameter glassy carbon working
169 electrode (BASi., UK), was also used. Before enzyme immobilization, GC electrodes were
170 mechanically polished with alumina and subsequently rinsed and sonicated in ultra pure deionized
171 water.

172 The P450 2D15 enzyme was immobilized on glassy carbon (GC) with two different approaches: a)
173 P450 2D15 entrapment in PDDA film by mixing equal volumes of 30 μM protein and surfactant
174 solutions before drop-coating on the electrode surfaces (GC/PDDA/2D15); b) P450 2D15
175 immobilization on GC electrodes using didodecyldimethylammonium bromide (DDAB) stabilized
176 gold nanoparticles (AuNPs) (GC/AuNPs/2D15). 5 μl of 5 mM colloidal gold in 0.1 M
177 DDAB/chloroform was placed on the electrode surface. After evaporation of the chloroform (10
178 min), 10 μl of 30 μM P450 2D15 solution was added onto the electrode surface. The electrodes
179 were kept overnight at 4 °C in a humid chamber to prevent their total drying.

180 Cyclic voltammetry experiments were carried out under anaerobic conditions in a glove box with <
181 5 ppm oxygen (Belle Technologies, UK). Cyclic voltammograms were collected between +100 and
182 -500 mV (vs Ag/AgCl) at a scan rate range of 20–120 mVs⁻¹ in the supporting electrolyte solution.
183 Electrocatalysis experiments were carried out using chronoamperometry applying a potential bias of
184 -650 mV (vs Ag/AgCl) or in cyclic voltammetry at 25°C in presence of metoprolol. The product
185 formed was separated and analyzed by HPLC as previously reported [38]. All electrocatalytic
186 experiments were carried out in triplicates and performed at 200 rpm rotation speed using a RDE-2
187 rotator system (BASi, USA).

188

189 ***2.6 HPLC analysis of electrocatalysis products***

190

191 After chronoamperometry in the presence of metoprolol substrate, electrocatalysis solution was
192 collected and an aliquot of 100 μL was injected in HPLC for product quantification.
193 Electrocatalysis products were identified by comparison of retention times to those obtained with
194 authentic standards. For this purpose, standard solutions of metoprolol, α-OH-metoprolol and O-
195 desmethyl-metoprolol were separated isocratically by HPLC (Agilent Technologies-1200 series,
196 Italy) coupled with diode array detector using a 4.6 × 150 mm 5 μm Eclipse XDB-C18 column
197 (Agilent Technologies, USA). Retention times were 3.8 min, 4.7 min and 10.5 min respectively for
198 α-OH-metoprolol, O-desmethyl-metoprolol and metoprolol.

199

200 **3. Results and discussion**

201 **3.1 Recombinant P450 2D15**

202

203 The gene coding for the full length cytochrome P450 2D15 was amplified from *Canis familiaris*
204 liver cDNA and three mutations were identified by full DNA sequencing. A silent substitution of an
205 adenine in guanine was found 325 bases after the 2D15 start with two other mutations leading to the
206 amino acid substitutions of Ile109Val and Phe115Leu in the full-length protein (g345c and g738a).
207 Cytochromes P450 variants in *C. familiaris* 2D15 are not unusual and have been previously
208 reported [28-30] as they are a consequence of the genetic variability existing between dog colonies
209 [39].
210

211 “Here Figure 1”

212
213 The gene encoding for the P450 2D15 variant with the three above-mentioned mutations was cloned
214 in the expression vector pCW and the OmpA leader peptide sequence was introduced at its N-
215 terminus to enhance the protein expression levels as described in the materials and methods. The
216 protein was heterologously expressed in *E. coli* and purified from the membrane fraction with a
217 yield of 4.1 mg of P450 per liter of culture. Cytochrome P450 2D15 (57 kDa) (Fig.1A) was purified
218 in presence of quinidine, a known inhibitor of human P450 2D6. The purified protein was also
219 stored in the presence of this inhibitor which has been shown to preserve the stability of the protein
220 [36]. The inhibitor was removed prior to each experimental assay through buffer exchange.
221 Contrary to all previous literature data, in this work the purified *C. familiaris* P450 2D15 protein
222 and not the microsomal or membrane-associated protein was studied.

223 Binding of carbon monoxide to the dithionite reduced protein confirmed the presence of the
224 correctly incorporated haem cofactor inside the protein scaffold. The protein in its oxidized form
225 presents a Soret peak at 417 nm, the α and β bands at 570 nm and 535 nm, respectively (Fig.1B). As
226 expected, the Soret peak shows the characteristic shift to 450 nm upon reduction and bubbling of
227 carbon monoxide due to the reduced and carbon monoxide-bound adduct and the α and β bands are
228 replaced by a single broad peak centered at 550 nm as shown in Fig.1B. Similarly to the
229 microsomal P450 2D15 reported by Roussel and colleagues [29], a partial amount of inactive
230 protein was also detected at 420 nm (Fig.1B).
231

232 **3.2 Direct electrochemistry of P450 2D15 on glassy carbon electrodes**

233 Recombinant P450 2D15 was immobilized on glassy carbon electrodes in a non-oriented fashion
234 either by entrapment within the cationic polymer polydiallyldimethylammonium chloride (PDDA)
235 (GC/PDDA/2D15) or in the presence of gold nanoparticles (AuNPs) (GC/AuNPs/2D15) which are
236 one of the most stable metal nanoparticles that provide an effective electron transfer to-and-from the
237 glassy carbon electrode [32, 40].

238 Once the protein was successfully immobilized on glassy carbon electrodes, cyclic voltammetry
239 experiments were carried out at 25°C under anaerobic conditions (< 5 ppm O₂) to prevent the
240 formation of the Fe²⁺-dioxygen complex related to the second electron transfer step within the
241 catalytic cycle of cytochromes P450. Cyclic voltammograms of P450 2D15 entrapped with PDDA
242 (GC/PDDA/2D15) or in presence of AuNPs (GC/AuNPs/2D15) are shown in Fig.2A and B,
243 respectively. In both cases the ratio between the anodic and cathodic peak currents were found to be
244 one but the magnitude of the current observed was nearly 4x higher in the presence of AuNPs. As
245 stated by Laviron’s theory [41], the linear dependence of the anodic and cathodic peak currents on
246 the scan rate (within the range 20-120 mV) for both GC/PDDA/2D15 and GC/AuNPs/2D15,
247 indicated that the electron transfer from/to the modified GC electrode is quasi-reversible and it is a
248 surface-controlled process as expected for an immobilized cytochrome P450 on electrode surfaces.
249

250 “Here Figure 2”

251

252 The resulting anodic and cathodic peak currents for GC/PDDA/2D15 were detected at -256 ± 6 mV
253 (Ea) and -127 ± 5 mV (Ec), respectively, with a calculated midpoint potential (Em) of -191 ± 5 mV
254 (vs Ag/AgCl). In the GC/AuNPs/2D15 immobilization strategy, the anodic and cathodic peak
255 currents were measured at -267 ± 5 mV (Ea) and -200 ± 4 mV (Ec) (Fig.2D) and the resulting
256 midpoint potential was calculated to be -233 ± 4 mV. These values are in the range of other
257 electrochemically determined midpoint potentials reported in the literature for different human
258 P450 enzymes [21].

259 Peak-to-peak separation value was calculated to be -129 ± 6 for GC/PDDA/2D15 and -67 ± 5 mV for
260 GC/AuNPs/2D15 indicating that the presence of the gold nanoparticles facilitates a much faster
261 electron transfer of P450 2D15 when immobilized on glassy carbon electrodes.

262 Apparent surface coverage of the electroactive protein was calculated from the slope of I_p versus v
263 plot in accordance with the Brown Anson model using the equation:

264

$$265 i_p = n^2 F^2 A \Gamma v / 4RT$$

266

267 where n represents the number of electrons involved in the reaction, A is the electrode surface area
268 (0.071 cm^2), Γ is the surface coverage, v is the scan rate, F is the Faraday constant, T is the
269 temperature and R is the gas constant. The surface coverage value on GC/PDDA was calculated to
270 be 1.1×10^{12} molecules/ cm^2 in the same range previously reported for the *Macaca fascicularis* P450
271 2C20 immobilized in the same manner [25]. As expected the same calculation of the surface
272 coverage in the presence of AuNps resulted in a value of 4.6×10^{12} molecules/ cm^2 , around 4 times
273 higher than using PDDA alone.

274 The electron transfer efficiency of the GC/AuNPs/2D15 was further investigated recording a series
275 of cyclic voltammograms varying the pH within the range $6.5 < \text{pH} < 8.5$ (Fig. 3). A negative shift in
276 peak potential upon lowering pH was observed which is indicative of proton-coupled electron
277 transfer [42]. The measured shift in the formal potential was around 60 mV per pH unit, close to the
278 theoretical value of 59 mV/pH expected at 25°C for one proton, one electron transfer. The
279 protonation site of the reduced P450 remains unknown but it is reasonable to assume that it is either
280 an amino acid in close proximity of the haem iron or the water bound in the sixth coordination, as
281 has been suggested in the case of other cytochromes P450 [42-43]. Nocera's group [44] have also
282 suggested that proton-coupled electron transfer in P450 enzymes is from a structured water, which
283 is the sixth coordinated H_2O mentioned above.

284

285 “Here Figure 3”

286

287

288 3.3 Electrocatalysis of 2D15 immobilized on glassy carbon electrodes

289

290 Electrocatalysis by the immobilized P450 2D15 (GC/AuNPs/2D15) was followed by both
291 chronoamperometry and cyclic voltammetry in the presence of metoprolol. The latter drug (Scheme
292 1) is a cardioselective β_1 -adrenergic blocking agent metabolized principally by the human P450
293 2D6 and converted into the α -OH-metoprolol and O-desmethyl-metoprolol products [38]. The
294 amount of O-desmethyl-metoprolol (scheme1-left) after electrocatalysis was found to be below the

295 detection limits. For this reason, only α -OH-metoprolol (scheme 1-right) was considered as a
296 product formed.

297

298

“Here Scheme 1”

299

300 As can be seen in Fig. 4A, a catalytic current was observed in air saturating conditions in the
301 presence of metoprolol in cyclic voltammetry experiments. Furthermore, using chronoamperometry
302 at regular intervals additions of metoprolol were carried out in the range of 12.5-250 μ M under
303 aerobic conditions (Fig. 4B) with an applied bias of -650 mV. The change in the
304 chronoamperometric currents registered due to the different concentrations of the drug showed a
305 Michaelis–Menten kinetic mechanism with a plateau or saturation at higher than 70 μ M
306 concentrations of metoprolol. The K_{Mapp} calculated from these currents was 39.5 \pm 3.5 μ M (Fig. 5A).

307

308

“Here Figure 4”

309

310 Further electrocatalysis experiments were carried out by chronoamperometry for both the
311 GC/AuNPs/2D15 and the GC/PDDA/2D15 systems applying a potential bias of -650 mV (vs
312 Ag/AgCl) for 30 min at 25 °C in presence of different concentrations of metoprolol (Fig. 5B). For
313 each concentration of the drug tested, the contents of the electrochemical cell were analyzed after
314 the 30 min reaction by HPLC in order to separate and quantify the product(s) formed by the
315 immobilized enzyme. No products were detected from the HPLC analysis for the *C. familiaris* P450
316 2D15 enzyme entrapped with the polycationic agent PDDA. On the other hand, the enzyme
317 immobilized in the presence of AuNps (GC/AuNPs/2D15) was capable of hydroxylating the
318 metoprolol producing 30.7 \pm 2.3 pmol of product at the higher metoprolol concentrations used. No
319 O-desmethylated product was observed in line with previously published data on microsomal P450
320 2D15 [28].

321

322

“Here Figure 5”

323

324 Control experiments were also carried out in the absence of the protein and as expected no product
325 was detected (data not shown). Quantification of the reaction products in the presence of increasing
326 amounts of metoprolol (Fig. 5B) resulted in a calculated apparent K_M value of 36.2 \pm 1.4 μ M for
327 GC/AuNPs/2D15 (Table 1) very similar to the K_{Mapp} obtained by titrating different concentrations
328 of metoprolol (see Fig. 5A). The electrochemically determined K_M values are also in the same range
329 as those reported by Ellis and colleagues for human P450 2D6 [45] therefore it can be concluded
330 that the *C. familiaris* P450 2D15 possesses similar enzymatic activity to human P450 2D6, at least
331 for metoprolol metabolism.

332

333

“Here Table 1”

334

335 4. Conclusions

336 The development of an electrochemical platform for the screening of animal cytochromes P450
337 represents an interesting and feasible solution to the ever increasing demand to reduce animal
338 testing, maintaining a high level of predictivity of the animal models used in preclinical tests and
339 providing the opportunity to study the P450 metabolism of new drugs and chemical entities.

340 To this end, the cloning of a new *Canis familiaris* P450 2D15 variant and its expression in a pure
341 form for its electrochemical application reported in this work, brings us a step closer to the

342 realization of an *in vitro* electrochemical toxicity screening, an alternative to *in vivo* animal testing
343 and sacrifice.

344 The P450 2D15 enzyme was successfully immobilized on glassy carbon electrodes in a stable form
345 achieving an efficient electron transfer between the electrode and the enzyme. The presence of gold
346 nanoparticles enhanced the sensitivity of the electrode-protein system and allowed for the
347 estimation of kinetic parameters for metoprolol, a typical drug marker of the human P450 2D6.

348 These results represent the first step towards the development of electrochemical platform for the
349 rapid exploration of the metabolic diversity existing between animals and humans cytochromes
350 P450 contributing to a more reliable interpretation of the data generated in canine species during the
351 pharmacological preclinical studies.

352

353

354 **ACKNOWLEDGEMENTS**

355 The authors wish to acknowledge financial support from the Regione Piemonte CIPE 2006
356 (CYPTECH-project, Italy) and Progetto Ateneo-San Paolo 2012 (awarded to S. Sadeghi).

357

358

359 **REFERENCES**

360

361 [1] M. Hudson-Shore. Statistics of Scientific Procedures on Living Animals 2012: another increase
362 in experimentation - genetically-altered animals dominate again. *Altern Lab Anim.* 41 (2013) 313-
363 319.

364

365 [2] O. Varga, A.K. Hansen, P. Sandøe, I.A. Olsson, Validating animal models for preclinical
366 research: a scientific and ethical discussion. *EMBO Rep.* 11 (2010) 500–503.

367

368 [3] J.E. May, J. Xu, H.R. Morse, N.D. Avent, C. Donaldson, Toxicity testing: the search for an in
369 vitro alternative to animal testing. *Br. J. Biomed. Sci.* 66 (2009) 160–165.

370

371 [4] L.M. Schechtman, W.S. Stokes. The FDA's regulatory role in the ICCVAM process. *Altern Lab*
372 *Anim.* (2004) 32, 663-668.

373

374 [5] C.A. Schuppli, D. Fraser, M. McDonald. Expanding the three Rs to meet new challenges in
375 humane animal experimentation. *Altern Lab Anim.* (2004) 32: 525-532.

376

377 [6] FP. Guengerich. Human cytochrome P450 enzymes. Ortiz de Montellano, P. R., editor. (2005)
378 *Cytochrome P450: Structure, Mechanism, and Biochemistry*, 3rd ed. pp. 377–463. Plenum, New
379 York.

380

381 [7] J.J. Bogaards, M. Bertrand, P. Jackson, M.J. Oudshoorn, R.J. Weaver, P.J. van Bladeren, B.
382 Walther. Determining the best animal model for human cytochrome P450 activities: a comparison
383 of mouse, rat, rabbit, dog, micropig, monkey and man. *Xenobiotica.* 30 (2000) 1131-52.

384

385 [8] J. Tibbitts. Issues related to the use of canines in toxicologic pathology--issues with
386 pharmacokinetics and metabolism. *Toxicol Pathol.* 31 (2003) 17-24.

387

388 [9] M. Martignoni, G.M. Groothuis, R. de Kanter. Species differences between mouse, rat, dog,
389 monkey and human CYP-mediated drug metabolism, inhibition and induction. *Expert Opin Drug*
390 *Metab Toxicol.* 6 (2006) 875-894.

391

392 [10] F. Rua, G. Di Nardo, SJ Sadeghi, G. Gilardi. Towards reduction in animal sacrifice for
393 drugs: Molecular modelling of *Macaca fascicularis* P450 2C20 for virtual screening of *Homo*
394 *sapiens* P450 2C8 substrates. *Biotechnol. Appl. Biochem.* (2012) 59, 479-489.

395

396 [11] M.N. Martinez, L. Antonovic, M. Court, M. Dacasto, J. Fink-Gremmels, B. Kukanich, C.
397 Locuson, K. Mealey, M.J. Myers, L. Trepanier. Challenges in exploring the cytochrome P450
398 system as a source of variation in canine drug pharmacokinetics. *Drug Metab Rev.* 45 (2013) 218-
399 230.

400

401 [12] S. Fleischer, M. Sharkey, K. Mealey, E.A. Ostrander, M. Martinez. Pharmacogenetic and
402 metabolic differences between dog breeds: their impact on canine medicine and the use of the dog
403 as a preclinical animal model. *AAPS* 10 (2008) 110-119.

404

405 [13] M. Mise, T. Hashizume, S. Komuro, Characterization of substrate specificity of dog CYP1A2
406 using CYP1A2-deficient and wild-type dog liver microsomes. *Drug Metab Dispos.* 36 (2008) 1903-
407 1908.

408
409 [14] C.W. Locuson, B.T. Ethell, M. Voice, D. Lee, K.L. Feenstra, Evaluation of Escherichia coli
410 membrane preparations of canine CYP1A1, 2B11, 2C21, 2C41, 2D15, 3A12, and 3A26 with co-
411 expressed canine cytochrome P450 reductase. *Drug Metab Dispos.* 37 (2009) 457-61.
412
413 [15] M. Shou, R. Norcross, G. Sandig, P. Lu, Y. Li, Y. Lin, Q. Mei, A.D. Rodrigues, T.H.
414 Rushmore, Substrate specificity and kinetic properties of seven heterologously expressed dog
415 cytochromes p450. *Drug Metab Dispos.* 31 (2003) 1161-1169.
416
417 [16] K.L. Mealey, M. Jabbes, E. Spencer, J.M. Akey. Differential expression of CYP3A12 and
418 CYP3A26 mRNAs in canine liver and intestine. *Xenobiotica.* 38 (2008) 1305-1312.
419
420
421 [17] V. Dodhia, C. Sassone, A. Fantuzzi, G. Di Nardo S.J. Sadeghi, G. Gilardi, Modulating the
422 coupling efficiency of human cytochrome P450 CYP3A4 at electrode surfaces through protein
423 engineering. *Electrochem. Commun.* 10 (2008) 1744–1747.
424
425
426 [18] A. Fantuzzi , E. Capria, L.H. Mak, V.R. Dodhia, S.J. Sadeghi, S. Collins, G. Somers, E. Huq,
427 G. Gilardi, An electrochemical microfluidic platform for human P450 drug metabolism profiling.
428 *Anal Chem.* 82 (2010) 10222-10227.
429
430 [19] S. Castrignanò, S.J. Sadeghi, G. Gilardi. Electro-catalysis by immobilised human flavin-
431 containing monooxygenase isoform 3 (hFMO3), *Anal Bioanal Chem*, 398 (2010), 1403-1409.
432
433
434 [20] S.J. Sadeghi, R. Meirinhos, G. Catucci, V.R. Dodhia, G. Di Nardo, G. Gilardi. Direct
435 electrochemistry of drug metabolizing human flavin-containing monooxygenase: electrochemical
436 turnover of benzydamine and tamoxifen, *J Am Chem Soc.* 132 (2010), 458-9.
437
438 [21] S.J. Sadeghi, A. Fantuzzi A, G. Gilardi. Breakthrough in P450 bioelectrochemistry and future
439 perspectives. *Biochim Biophys Acta.* 1814 (2011) 237-248.
440
441 [22] S. Castrignanò, A. Ortolani, S.J. Sadeghi, G. Di Nardo, P. Allegra, G. Gilardi. Electrochemical
442 detection of human cytochrome P450 2A6 inhibition: a step toward reducing dependence on
443 smoking. *Anal.Chem.* 86 (2014) 2760-2766.
444
445 [23] D.L. Johnson, A.J. Conley, L.L. Martin. Direct electrochemistry of human, bovine and porcine
446 cytochrome P450c17. *J Mol Endocrinol.* 36 (2006) 349-359.
447
448 [24] V.V. Shumyantseva, T.V. Bulko, T.T. Bachmann, U. Bilitewski, R.D. Schmid, A.I. Archakov.
449 Electrochemical reduction of flavocytochromes 2B4 and 1A2 and their catalytic activity. *Arch*
450 *Biochem Biophys.* 377 (2000) 43-48.
451
452 [25] F. Rua, S.J. Sadeghi, S. Castrignanò, G. Di Nardo, G. Gilardi. Engineering *Macaca fascicularis*
453 cytochrome P450 2C20 to reduce animal testing for new drugs. *J Inorg Biochem.* 117 (2012) 277-
454 284.
455

- 456 [26] S.F. Zhou, Polymorphism of human cytochrome P450 2D6 and its clinical significance: Part I.
457 Clin Pharmacokinet. 48 (2009) 689-723.
458
- 459 [27] Neafsey P, Ginsberg G, Hattis D, Sonawane B. Genetic polymorphism in cytochrome P450
460 2D6 (CYP2D6): Population distribution of CYP2D6 activity. J Toxicol Environ Health B Crit Rev.
461 12 (2009) 334-361.
462
- 463 [28] K. Sakamoto, S. Kirita, T. Baba, Y. Nakamura, Y. Yamazoe, R. Kato, A. Takanaka, T.
464 Matsubara, A new cytochrome P450 form belonging to the CYP2D in dog liver microsomes:
465 purification, cDNA cloning, and enzyme characterization. Arch Biochem Biophys. 1 (1995) 372-82.
466
- 467 [29] F. Roussel, D.B. Duignan, M.P. Lawton, R.S. Obach, C.A. Strick, D.J. Tweedie, Expression
468 and characterization of canine cytochrome P450 2D15. Arch Biochem Biophys. 357 (1998) 27-36.
469
- 470 [30] T. Tasaki, H. Iwata, A. Kazusaka, S. Fujita, Regio- and stereoselectivity in propranolol
471 metabolism by dog liver microsomes and the expressed dog CYP2D15. J Biochem. 123 (1998) 747-
472 751.
473
- 474 [31] S. Guo, E. Wang. Synthesis and electrochemical applications of gold nanoparticles. Anal.
475 Chim. Acta. 598 (2007) 181-192.
476
- 477 [32] S. Castrignanò, S.J. Sadeghi, G. Gilardi. Entrapment of human flavin-containing
478 monooxygenase 3 in the presence of gold nanoparticles: TEM, FTIR and electrocatalysis. Biochim
479 Biophys Acta. 1820 (2012) 2072-2078.
480
- 481 [33] EM. Gillam, Z. Guo, FP Guengerich. Expression of modified human cytochrome P450 2E1 in
482 Escherichia coli, purification, and spectral and catalytic properties. Arch. Biochem. Biophys 312
483 (1994), 59-66.
484
- 485 [34] M.P. Pritchard, M.J. Glancey, J.A. Blake, D.E. Gilham, B. Burchell, C.R. Wolf, T. Friedberg,
486 Functional co-expression of CYP2D6 and human NADPH-cytochrome P450 reductase in
487 Escherichia coli. Pharmacogenetics. 8 (1998) 33-42.
488
- 489 [35] P. Panicco, VR Dodhia, A. Fantuzzi, G. Gilardi. First enzyme-based amperometric platform to
490 determine the polymorphic response in drug metabolism by cytochromes P450, Anal. Chem. 83
491 (2011) 2179-2186.
492
- 493 [36] K. Berka, E. Anzenbacherová, T. Hendrychová, R. Lange, V. Mašek, P. Anzenbacher, M.
494 Otyepka. Binding of quinidine radically increases the stability and decreases the flexibility of the
495 cytochrome P450 2D6 active site. J Inorg Biochem. 110 (2012) 46-50.
496
- 497 [37] T. Omura, R. Sato, The Carbon Monoxide-Binding Pigment of Liver Microsomes. I. Evidence
498 for Its Hemoprotein Nature. J Biol Chem 239 (1964) 2370-8.
499
- 500 [38] I.H. Hanna, J.A. Krauser, H. Cai, M.S. Kim, F.P. Guengerich. Diversity in mechanisms of
501 substrate oxidation by cytochrome P450 2D6. Lack of an allosteric role of NADPH-cytochrome
502 P450 reductase in catalytic regioselectivity. J Biol Chem. 276 (2001) 39553-395561.
503

504 [39] M.N. Martinez, L. Antonovic, M. Court, M. Dacasto, J. Fink-Gremmels, B. Kukanich, C.
505 Locuson, K. Mealey, M.J. Myers, L. Trepanier. Challenges in exploring the cytochrome P450
506 system as a source of variation in canine drug pharmacokinetics. *Drug Metab Rev.* 45 (2013) 218-
507 230.
508
509 [40] R. Sardar, A.M. Funston, P. Mulvaney, R.W. Murray. Gold nanoparticles: past, present, and
510 future. *Langmuir.* 15 (2009) 13840-13851.
511
512 [41] E. Laviron, General expression of the linear potential sweep voltammogram in the case of
513 diffusionless electrochemical systems. *J. Electroanal. Chem.* 101 (1979) 19-28.
514
515 [42] B.D. Fleming, S.G. Bell, L-L. Wong, A.M. Bard, The electrochemistry of a heme-containing
516 enzyme, CYP199A2, adsorbed directly onto a pyrolytic graphite electrode, *J. Electroanal. Chem.*
517 611 (2007) 149-154.
518
519 [43] A. Shukla, E.M. Gillam, D.J. Mitchell, P.V. Bernhardt, Direct electrochemistry of enzymes
520 from the cytochrome P450 2C family, *Electrochem. Commun.* 7 (2005) 437-442.
521
522 [44] S.Y. Reece, J.M. Hodgkiss, J. Stubbe, D.G. Nocera, Proton-coupled electron transfer: the
523 mechanistic underpinning for radical transport and catalysis in biology, *Phil. Trans. R. Soc. B* 361
524 (2006) 1351-1364.
525
526 [45] S.W. Ellis, K. Rowland, M.J. Ackland, E. Rekka, A.P. Simula, M.S. Lennard, C.R. Wolf, G.T.
527 Tucker. Influence of amino acid residue 374 of cytochrome P-450 2D6 (CYP2D6) on the regio- and
528 enantio-selective metabolism of metoprolol. *Biochem J.* 316 (1996) 647-654.
529
530
531

532 **Figure legends:**

533

534 **Fig. 1:** Purification and spectral characterization of P450 2D15. (A) SDS-PAGE gel, lane 1:
535 molecular weight markers, lane 2: purified protein (57 kDa). The absorbance spectra of the purified
536 P450 2D15 (B) in the oxidized (solid black line), dithionite reduced (dotted line), and the reduced
537 carbon monoxide-bound form (dashed line).

538

539 **Fig. 2:** Electrochemical characterization of P450 2D15 immobilized on glassy carbon electrodes
540 (A) entrapped with the cationic surfactant PDDA (GC/PDDA/2D15), and (B) in presence of gold
541 nanoparticles (GC/AuNPs/2D15). Cyclic voltammogram of P450 2D15 measured at a scan rate of
542 120 mV/s in 50 mM potassium phosphate buffer pH 7.4 with 100 mM KCl at 25 °C. Shown are the
543 original and baseline corrected (upper traces) cyclic voltammograms. Bottom: plot of cathodic
544 (filled symbols) and anodic (empty symbols) peak currents versus scan rate. $R^2 > 0.99$.

545

546 **Fig. 3:** Cyclic voltammograms of GC/AuNPs/2D15 at a scan rate of 120 mVs⁻¹ under anaerobic
547 conditions in different pH value buffer. The cyclic voltammogram at pH 7.4 is shown in black.

548

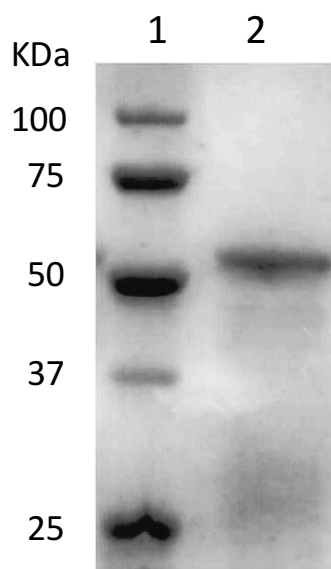
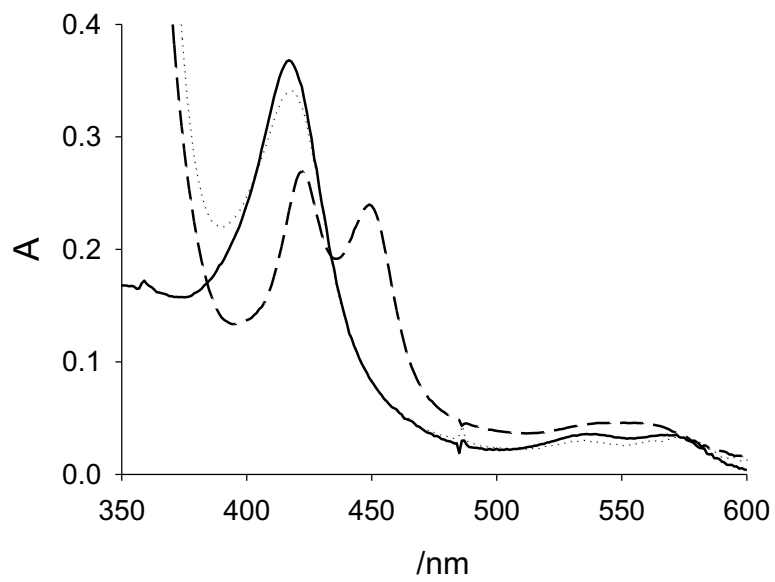
549 **Fig. 4:** Electrochemical responses of GC/AuNPs/2D15 to metoprolol. (A) Cyclic voltammograms
550 of the GC/AuNPs/2D15 in the air-saturated buffer in presence (black) and absence (grey) of
551 metoprolol shown together with control trace obtained in the absence of the protein (dashed); (B)
552 Chronoamperometric response of GC/AuNPs/2D15 at -650 mV followed for 600 sec in 50 mM
553 potassium phosphate buffer pH 7.4. The arrows indicate the addition of different concentrations of
554 metoprolol (12.5-250 μM).

555

556 **Fig. 5:** Michaelis–Menten plot of the turnover of P450 2D15 immobilized on glassy carbon
557 electrode in presence of AuNps (GC/AuNPs/2D15) and metoprolol obtained from: (A) the current
558 registered in the titration experiments (Δ: current increase upon metoprolol addition) and, (B)
559 product quantified by HPLC after 30 min electrocatalysis.

560

561

A**B****Figure 1**562
563

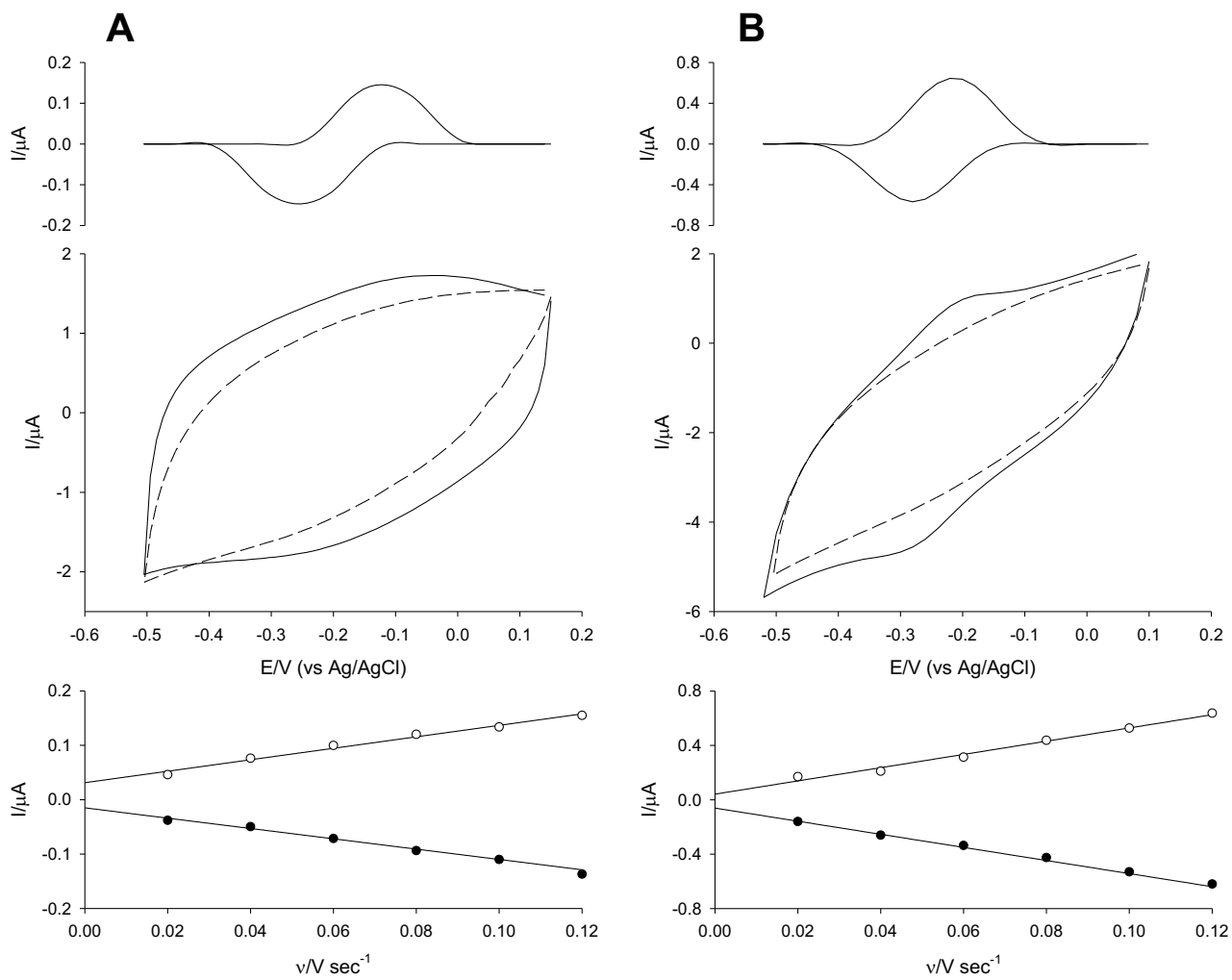


Figure 2

564
565

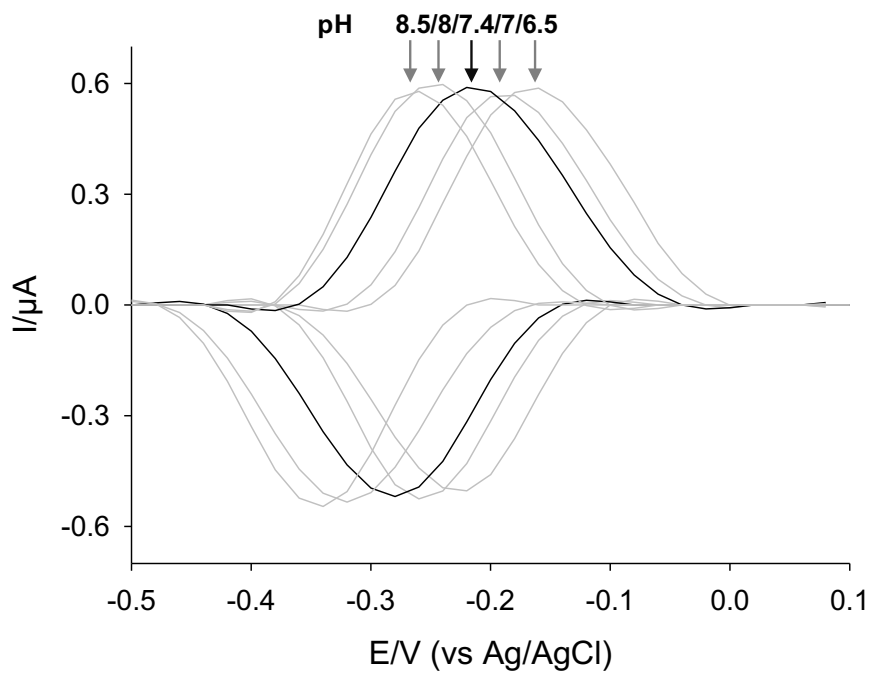
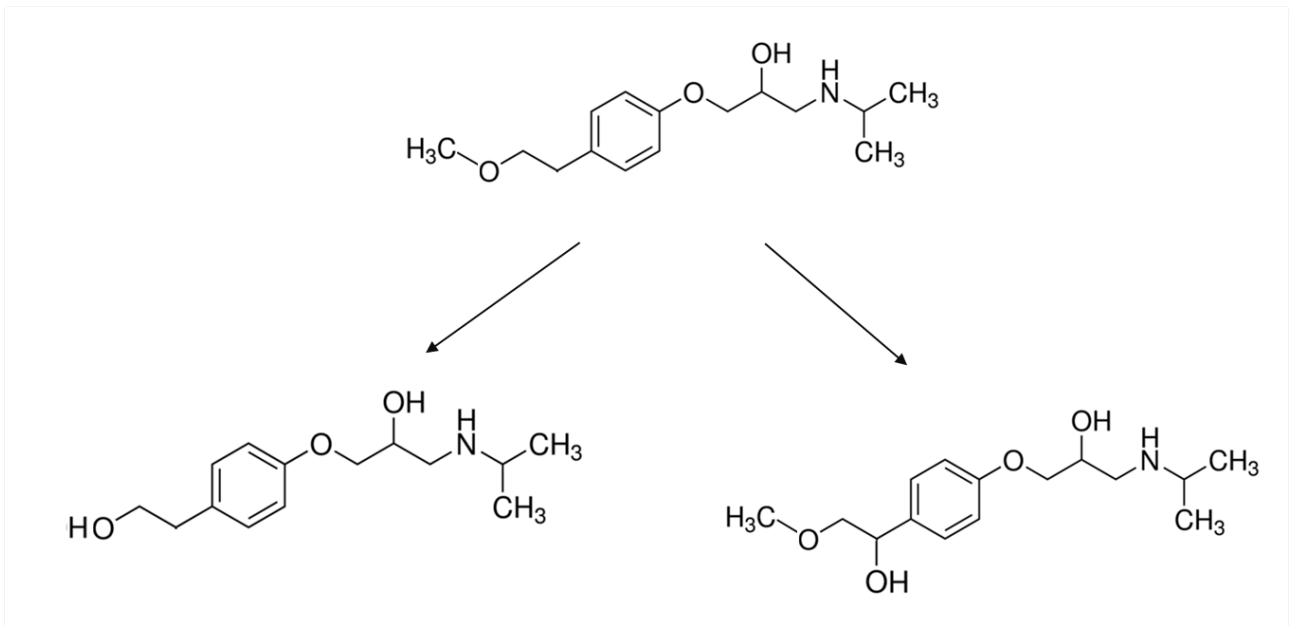


Figure 3

566
567



Schematic 1

568
569

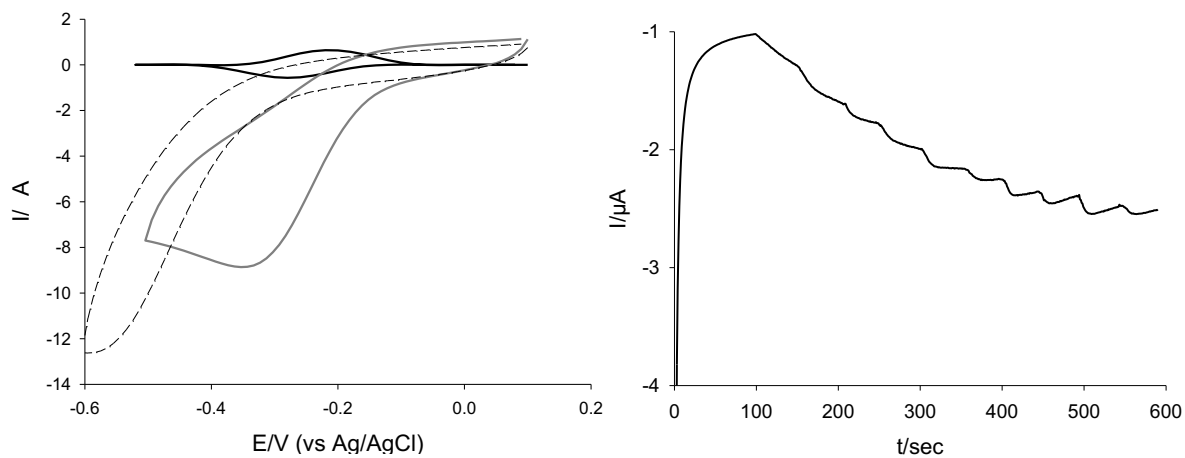


Figure 4

570
571

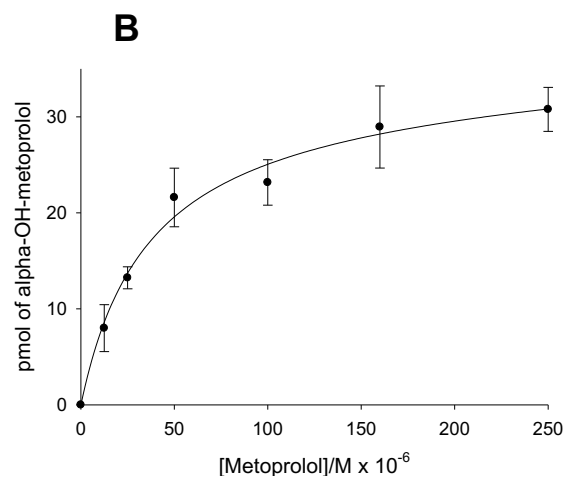
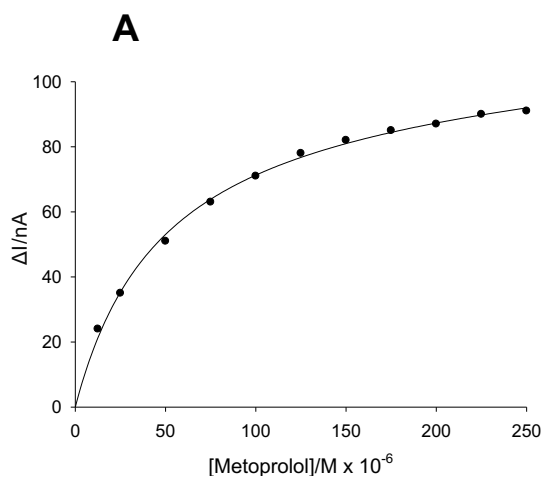


Figure 5